

Hemocompatibility Assessment Platform Drive System Design: Trade-off between Motor Performance and Hemolysis*

Shweta Karnik, P. Alex Smith, Eiji Ogiwara, Charles D. Fraser, Jr., O. H. Frazier, Nobuyuki Kurita,
Katharine H. Fraser, and Yaxin Wang, *Member, IEEE*

Abstract— Left ventricular assist devices (LVADs) have long been used to treat adults with heart failure, but LVAD options for pediatric patients with heart failure are lacking. Despite the urgent need for long-term, implantable pediatric LVADs, design challenges such as hemolysis, pump thrombosis, and bleeding persist. We have developed a Hemocompatibility Assessment Platform (HAP) to identify blood trauma from individual LVAD components. A HAP would aid in refining pump components before in vivo testing, thereby preventing unnecessary animal sacrifice and reducing development time and cost. So that the HAP does not confound hemolysis data, the HAP drive system consists of an enlarged air-gap motor coupled to a magnetic levitation system. Although it is known that an enlarged air gap motor will have diminished performance, while the larger gap in the motor will cause less blood damage, the trade-offs are not fully characterized. Therefore, in this study we evaluated these trade-offs to determine an optimal rotor diameter for the HAP drive motor. The motor performance was characterized with an experimental method by determining the torque constant for the HAP drive motor with varied rotor diameters. The torque threshold was set as 10 mNm to achieve a nominal current of 3.5A. Hemolysis in the HAP drive motor gap was estimated by calculating scalar shear stress generated in the HAP motor gap analytically and numerically. A design criterion of 30 Pa was selected for scalar shear stress to achieve minimal hemolysis and platelet activation in the HAP drive system.

Clinical Relevance— We evaluated a Hemocompatibility Assessment Platform for developing LVAD prototypes that can best balance motor performance and hemocompatibility. This design method can assist with optimizing the drive system during the research stage and illustrates how motor geometry can be tuned to reduce blood trauma.

I. INTRODUCTION

Heart failure is the one of the leading causes of death in the United States. According to National Health and Nutrition Examination Survey data collected from 2013-2016, approximately 6.2million American adults suffer from heart failure [1]. Left ventricular assist devices (LVADs) are used for bridge-to-transplant, destination therapy, and bridge-to-

recovery for patients with heart failure [2]. Despite clinical success in adults, the options for LVAD use in small children are limited [3], and designing a new LVAD for long-term operation without causing hemolysis, pump thrombosis, and bleeding remains challenging [4], [5].

We have developed a Hemocompatibility Assessment Platform (HAP) to evaluate the blood trauma caused by individual LVAD components and to inform LVAD design [6]. The HAP can be used to identify the contribution of each component to the overall hemocompatibility of developmental LVADs, including contributions to hemolysis, platelet activation, and von Willebrand factor cleavage [7]. This enables rapid iterative testing to optimize pump structures before manufacturing and assembling an entire LVAD, or even before designing the device.

One essential part of the HAP is its drive system: a motor with a fully magnetically levitated rotor (accomplished by a magnetic levitation bearing) (Fig. 1). By eliminating contact bearings, this design has the potential to minimize blood trauma, once optimized. A crucial part of the optimization is reducing shear stress in the motor gap. Because a high rotational speed (15,000-20,000 rpm) is required for some testing scenarios, the only way to reduce shear stress is to increase the gap between the motor rotor and motor stator. General-purpose brushless direct current (BLDC) motors of the size required for this application (outer diameter of 22 mm) typically have an air gap of approximately 0.1mm. Based on the analytical estimation for the index of hemolysis (IH) correlation from Zhang et. al [8], the blood will repeatedly be exposed to high shear stress (>100 Pa). However, the shear

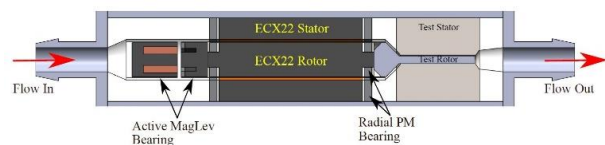


Figure 1. Hemocompatibility assessment platform

*Research supported by the National Heart, Lung, and Blood Institute of the National Institute of Health under Award Number 1R01HL153538-01.

Shweta Karnik is with Innovative Device and Engineering Applications, Texas Heart Institute, Houston, TX 77030 USA. (office: 832-355-9470; fax: 832-355-9552; e-mail: skarnik@texasheart.org).

P. Alex Smith is with Innovative Device and Engineering Applications, Texas Heart Institute, Houston, TX 77030 USA. (e-mail: palxs@gmail.com).

Eiji Ogiwara is with the Department of Electronics and Informatics, Gunma University, Gunma, Japan (e-mail: t170d507@gunma-u.ac.jp).

Charles Fraser is with the Division of Pediatric and Congenital Cardiothoracic Surgery and Cardiothoracic Surgery, The University of Texas

at Austin, Austin, TX 78705 USA. (e-mail: Charles.Fraser@austin.utexas.edu).

O. H. Frazier is with the Center for Preclinical Surgical & Interventional Research, Texas Heart Institute, Houston, TX 77030 USA. (e-mail: OFrazier@texasheart.org).

Nobuyuki Kurita is with the Department of Electronics and Informatics, Gunma University, Gunma, Japan (e-mail: nkurita@gunma-u.ac.jp).

Katharine Fraser is with the Mechanical Engineering Department, University of Bath, Bath, United Kingdom. (e-mail: khf27@bath.ac.uk).

Yaxin Wang is with Innovative Device and Engineering Applications, Texas Heart Institute, Houston, TX 77030 USA (e-mail: ywang@texasheart.org).

stress threshold for platelet activation in implantable LVADs is set at 50 Pa [9], [10]. Therefore, an enlarged motor gap is required for the HAP drive system. However, increasing the motor gap can compromise motor performance, resulting in inadequate motor torque to drive the entire system [11]. An optimal motor gap must be large enough to avoid generating high shear without being so large as to stunt motor function.

In this study, we experimentally evaluated the motor performance and analytically and numerically evaluated the fluid flow properties causing hemolysis. Dynamic performance of a set of BLDC motors with varied rotor outer diameter (OD) was measured by using a validated dynamometer, and shear stress in the gap was modeled by using computational fluid dynamics. The trade-offs were then evaluated to determine the rotor OD range for the HAP drive system that can best balance the HAP's motor performance and induced hemolysis.

II. MATERIALS AND METHODS

A. Motor Performance Characterization

An ECX22 commercial BLDC motor (Maxon Precision Motors, Inc., Taunton, MA, USA) was used for the HAP drive system. Our previous work [12] indicates that approximately 1.5 mNm of torque is required for the motor to achieve a target flow of 2 L/min at a 90-mmHg pressure head in a miniature LVAD. For safety reasons, a torque threshold of 10 mNm was set to achieve the ECX22 motor's nominal current (3.5 A).

Fig. 2 shows the experimental setup for performance characterization of the ECX22 BLDC motor. The rotor OD was varied from 6.5 mm to 10 mm at 0.5-mm increments. A motor was mounted on the jig and coupled to a torque meter (TB-200NM; Sugawara Laboratories, Inc, Kanagawa, Japan). A torque controller (DMC-2; Sugawara Laboratories, Inc.) applied a brake torque (σ) of 10 mNm. The ECX22 motor was driven at a specified 20,000 rpm by a pulse-width modulation amplifier (S24V10A-H3; Koford Engineering, LLC, Winchester, OH, USA), and motor speed (ϵ) was recorded. The terminal box connected the power meter (WT-1800; Yokogawa Test & Measurement, Tokyo, Japan) to the ECX22 motor and pulse-width modulation amplifier. The motor current (I) and voltage (U) were recorded for eight motor geometries.

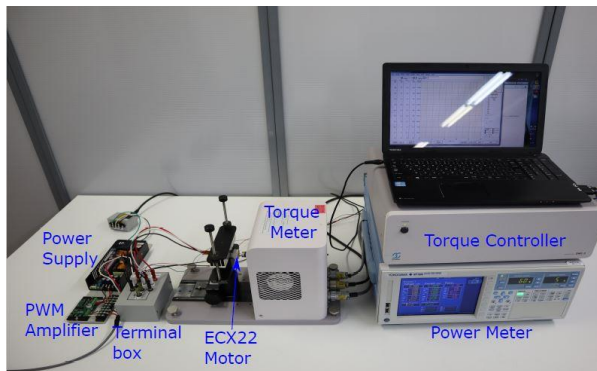


Figure 2. Experimental setup for motor performance testing

The motor performance was assessed by calculating the torque constant, K_T :

$$K_T = \frac{\sigma}{I} \text{ mNmA}^{-1} \quad (1)$$

B. In Silico Hemolysis Estimation

The hemolysis induced in the HAP motor gap was estimated by calculating the scalar shear stress (SSS) analytically and numerically. A design criterion of 30 Pa was selected for SSS to achieve minimal hemolysis and platelet activation in the HAP drive system.

1) Geometry and Meshing

Based on Fig. 1, a 3D geometry for the blood flow in the HAP drive motor gap (Fig. 3) was modeled by using Design Modeler software (Ansys, Inc, Canonsburg, PA, USA). The fluid domain was divided into three regions: (1) entrance (length 200 mm), (2) concentric radial gap (length 37.9 mm), and (3) exit (length 50 mm). The stator OD was set to 10.7 mm, whereas the rotor OD was varied from 6 mm to 10 mm at 1-mm increments. The entrance and the exit region enabled fully developed flow.

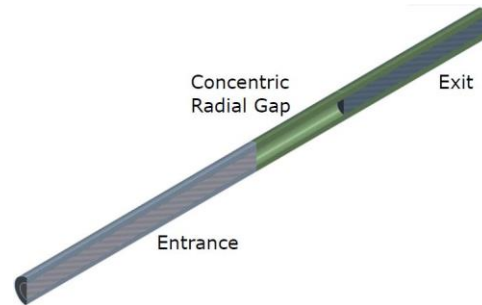


Figure 3. 3D geometry of HAP drive motor gap for in silico hemolysis evaluation

The HAP fluid domain was discretized with conformal interfaces. The concentric radial gap region consisted of a structured mesh with hexahedral element concentration at the rotor-stator boundaries. The entrance and exit regions were meshed with a combination of a structured and an unstructured mesh of element size 0.005 m. Three meshes consisting of 500K, 1M, and 2M elements with same structure were produced to analyze grid independence.

2) Analytical Shear Stress

Shear stress in the HAP motor gap was first estimated analytically, assuming Couette flow conditions:

$$\sigma = \mu \frac{\Delta v}{\Delta R} \quad (2)$$

where μ is the dynamic viscosity of blood at 0.0035 Pa s, Δv is the change in linear speed, m/s, and ΔR is the radial gap size, m.

3) Computational Fluid Dynamics

Taylor numbers ranged from 8×10^4 to 1.45×10^7 , which indicated complex turbulent flows in the HAP motor gap [13]. Therefore, the unsteady Reynolds Averaged Navier-Stokes equations were solved by using Fluent 2021R1 (Ansys, Inc.).

Blood was defined as an incompressible Newtonian fluid with a density of 1050 kg/m³ and a dynamic viscosity of 0.0035 kg/m-s. Boundary conditions included uniform

velocity at the inlet and constant pressure at the outlet. The inlet velocity was chosen to give flow rates in the range 100-300 mL/min. The HAP rotor wall was set to rotate at 20,000 rpm, and the stator has no-slip stationary wall conditions. The time step size was 1.67×10^{-5} s, which is equivalent to a 2° rotation per time step. The $k-\omega$ shear stress transport (SST) model was selected for turbulence closure [14].

The SSS for the radial HAP gap was calculated from the Computational Fluid Dynamics (CFD) results by using a User-Defined Function based on the following equation [15]:

$$\sigma = \left[\frac{1}{6} \sum (\sigma_{ii} - \sigma_{jj})(\sigma_{ii} - \sigma_{jj}) + \sum (\sigma_{ij}\sigma_{ij}) \right]^{1/2} \quad (3)$$

A convergence criterion of 10^{-5} was assigned to the residuals for each time step. The simulation was set to run until the volume averaged SSS was constant with time ($\sim 8,100$ time steps).

4) Hemolysis Calculation

The hemocompatibility of the HAP was evaluated by using the IH calculated from both the analytical shear stress and volume-averaged SSS, and average time in the motor by using a power law model as below, with coefficients as determined by Zhang, et al. [8].

$$IH(\%) = 1.228 \times 10^{-5} (t^{1.9918}) (\sigma^{0.6606}) \quad (4)$$

where t is the average time in the motor calculated from the flow rate, s , and σ is the shear stress produced in the HAP, Pa.

III. RESULTS

A. Motor Performance Characterization

The motor performance of the HAP drive motor was characterized by using torque constant calculated experimentally from Equation (1), as shown in Fig. 4. As the rotor OD increased from 6.5 mm to 10.0 mm, the torque constant increased from 1.90 mNm/A to 3.82 mNm/A, and the motor current decreased from 5.2 A to 2.6 A. As per the ECX22 BLDC motor specifications sheet, the nominal current is about 3.5A, which means that the minimal torque constant requirement is 2.86 mNm/A for this application. Therefore, a rotor OD larger than 8.0 mm meets the design requirement.

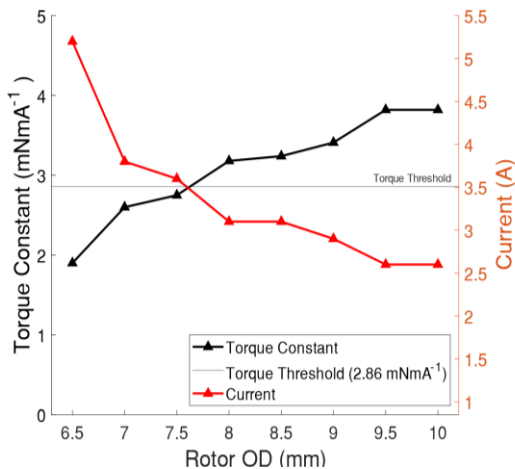


Figure 4. Torque constant and current generated at 20,000 rpm by ECX22 motor with varied rotor OD

B. In Silico Hemolysis Estimation

The SSS generated in the HAP drive motor radial gap was calculated analytically and numerically. We found that SSS increased as rotor OD increased (Fig. 5); for example, at 200 mL/min, the SSS increased from 11.91 Pa to 117.1 Pa numerically, whereas it increased from 9.36 Pa to 104.72 Pa analytically. The difference between numerical and analytical results was approximately 27%. For any rotor OD, the SSS decreased negligibly with the increase in flow rate. As the design criterion of SSS was set at 30 Pa for good hemocompatibility, the rotor OD cannot exceed 8.0 mm, as seen in Fig. 5.

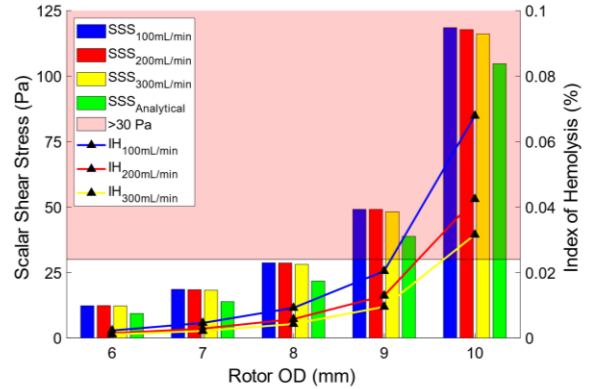


Figure 5. Scalar shear stress and index of hemolysis produced in the varied HAP motor gap.

The IH was calculated by substituting average time of blood in the motor and SSS generated in HAP in Equation (4). The IH increased as the rotor OD increased. The result indicates that with the rotor OD at 8.0 mm, the single-pass IH increased from 0.004% to 0.009% when the flow rate increased from 100 mL/min to 300 mL/min.

IV. DISCUSSION

A. Motor Performance Characterization

The HAP drive motor performance was characterized by using experimental methods. The torque constant was calculated for eight motor geometries with varied rotor ODs by using Equation (1). In our previous work [6], a numerical model for the ECX22 motor was established by using the finite element method in COMSOL v5.3a simulation software. The torque constant was also calculated numerically for the ECX22 motor, with varied rotor ODs. A difference between the numerical and experimental results was observed. One possible explanation is that, in the numerical model, the phase difference between the rotating magnetic field and the motor's permanent magnet was assumed to be 90° (i.e., peak performance), which gave a higher value for the torque constant, whereas the experimental setup could not control the phase difference between the rotating magnetic field and the motor's permanent magnet.

B. In Silico Hemolysis Estimation

Hemolysis induced in the HAP drive system was evaluated numerically. The SSS in the ECX22 motor with varied rotor ODs was calculated analytically by using Equation (2). A numerical CFD model was established to simulate the blood

flow in the ECX22 motor radial gap; blood damage was quantified by using Equations (3) and (4). The error between the analytical and numerical results can be explained by the presence of Taylor vortices in the ECX22 motor radial gap. The effect of flow rate on SSS was negligible, due to the higher circumferential velocity gradient versus the axial velocity gradient across the gap, although we qualitatively observed that the formation of Taylor vortices was “pushed back” by higher flow rates (Fig. 6). This model can be used to estimate the hemocompatibility of a HAP drive system with varied rotor ODs and to select the HAP drive system design for future study.

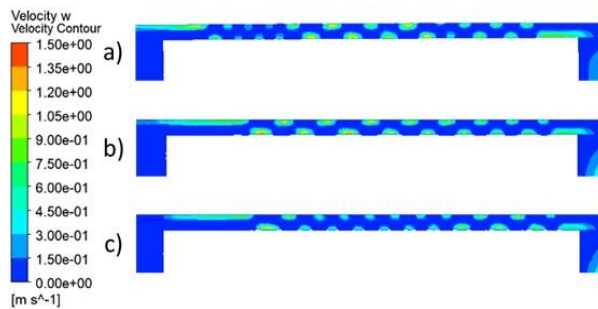


Figure 6. Formation of Taylor vortices in the HAP motor gap at a) 100 mL/min, b) 200 mL/min, and c) 300 mL/min

C. Trade-off Between Motor Performance and Hemolysis

In this study, we analyzed the trade-off between motor performance and hemolysis induced in the HAP drive system with varied rotor ODs. As seen from the motor performance characterization (Fig. 4), a larger rotor OD produces higher torque at a lower input current, but the hemolysis evaluation (Fig. 5) suggests that higher SSS is generated with a larger rotor OD. An optimal balance between the motor performance and the hemocompatibility of the HAP drive system was achieved by selecting a rotor OD of 8.0 mm. The next step toward validating this design approach will be to manufacture the HAP motor system and evaluate its hemocompatibility in an in vitro blood test loop.

V. CONCLUSION

We measured the performance of the HAP drive motor with varied rotor ODs and established a CFD model for predicting induced hemolysis in the system. To select the prototype that can best balance motor performance and hemocompatibility for the HAP, the IH was estimated with varied rotor ODs and flow rates. A rotor OD of 8 mm was selected for the HAP drive system to meet the torque requirement while inducing minimal hemolysis and platelet activation. This design method can assist with optimizing the drive system during the research stage and illustrates how motor geometry can be tuned to reduce blood trauma.

The next step in HAP development is to manufacture and assemble the drive system.

ACKNOWLEDGMENT

The authors thank Jeanie F. Woodruff, BS ELS, of the Department of Scientific Publications at the Texas Heart Institute, for her editorial contributions.

REFERENCES

- [1] E. J. Benjamin, P. Muntner, A. Alonso, et al., "Heart Disease and Stroke Statistics-2019 Update: A Report From the American Heart Association," *Circulation*, vol. 139, pp. e56-e528, 2019.
- [2] S. G. Drakos, A. G. Kfoury, J. Stehlik, et al., "Bridge to Recovery: Understanding the Disconnect Between Clinical and Biological Outcomes," *Circulation*, vol. 126, pp. 230-241, 2012.
- [3] I. Adachi and C. D. Fraser, "Mechanical circulatory support for infants and small children," presented at Seminars in Thoracic and Cardiovascular Surgery: Pediatric Cardiac Surgery Annual, 2011.
- [4] P. M. Eckman and R. John, "Bleeding and Thrombosis in Patients With Continuous-Flow Ventricular Assist Devices," *Circulation*, vol. 125, pp. 3038-3047, 2012.
- [5] C. Heilmann, U. Geisen, C. Benk, et al., "Haemolysis in patients with ventricular assist devices: major differences between systems☆," *European journal of cardio-thoracic surgery*, vol. 36, pp. 580-584, 2009.
- [6] Y. Wang, S. Karnik, P. A. Smith, A. Elgalad, O. H. Frazier, and N. Kurita, "Numerical and experimental approach to characterize a BLDC motor with different radial-gap to improve hemocompatibility performance," *Annu Int Conf IEEE Eng Med Biol Soc*, vol. 2020, pp. 2662-2666, 2020.
- [7] C. H. H. Chan, I. L. Pieper, S. Fleming, et al., "The effect of shear stress on the size, structure, and function of human von Willebrand factor," *Artificial organs*, vol. 38, pp. 741-750, 2014.
- [8] T. Zhang, M. E. Taskin, H. B. Fang, et al., "Study of Flow-Induced Hemolysis Using Novel Couette-Type Blood-Shearing Devices," *Artificial organs*, vol. 35, pp. 1180-1186, 2011.
- [9] B. Thamsen, B. Blümel, J. Schaller, et al., "Numerical analysis of blood damage potential of the HeartMate II and HeartWare HVAD rotary blood pumps," *Artif Organs*, vol. 39, pp. 651-9, 2015.
- [10] K. H. Fraser, T. Zhang, M. E. Taskin, B. P. Griffith, and Z. J. Wu, "A quantitative comparison of mechanical blood damage parameters in rotary ventricular assist devices: shear stress, exposure time and hemolysis index," *J Biomech Eng*, vol. 134, pp. 081002, 2012.
- [11] Y. Wang, T. G. Logan, P. A. Smith, et al., "Systematic Design of a Magnetically Levitated Brushless DC Motor for a Reversible Rotary Intra-Aortic Blood Pump," *Artificial Organs*, pp. n/a-n/a, 2017.
- [12] P. A. Smith, Y. Wang, S. A. Bieritz, et al., "Design Method Using Statistical Models for Miniature Left Ventricular Assist Device Hydraulics," *Annals of biomedical engineering*, vol. 47, pp. 126-137, 2019.
- [13] K. H. Fraser, M. E. Taskin, B. P. Griffith, and Z. J. Wu, "The use of computational fluid dynamics in the development of ventricular assist devices," *Medical Engineering & Physics*, vol. 33, pp. 263-280, 2011.
- [14] F. R. Menter, "Two-equation eddy-viscosity turbulence models for engineering applications," *ALAA journal*, vol. 32, pp. 1598-1605, 1994.
- [15] C. Bludszweit, "Three-Dimensional Numerical Prediction of Stress Loading of Blood Particles in a Centrifugal Pump," *Artificial organs*, vol. 19, pp. 590-596, 1995.